Compact ellipsometer employing a static polarimeter module with arrayed polarizer and wave-plate elements

Takashi Sato,[1] Takeshi Araki,[1] Yoshihiro Sasaki,[2] Toshihide Tsuru,[3] Toshiyasu Tadokoro,[1] and Shojiro Kawakami[1,3]

[1]Photonic Lattice, Inc., Aoba Incubation Square, Aoba, Aramaki, Aoba-ku, Sendai 980-0845, Japan
[2]Graduate School of Engineering, Tohoku University, Aoba, Arakami, Aoba-ku, Sendai 980-8579, Japan
[3]SFAIS, Aoba Incubation Square, Aoba, Aramaki, Aoba-ku, Sendai 980-0845, Japan

*Corresponding author: sato@photonic-lattice.com

Received 23 October 2006; revised 16 April 2007; accepted 22 April 2007;
posted 24 April 2007 (Doc. ID 75758); published 6 July 2007

A portable ellipsometer with a compact static polarimeter using an arrayed polarizer, an arrayed wave plate, and a CCD image sensor is developed. A high level of repeatability at a measurement speed of 0.3 s is demonstrated by measurement of SiO_2 films ranging from 2 to 300 nm in thickness deposited on an Si wafer. There is the potential to realize an ultracompact ellipsometer module by integrating the optical source and receiver, suitable for deployment in a variety of manufacturing equipment and measurement instruments. © 2007 Optical Society of America

OCIS codes: 120.2130, 120.5410.

1. Introduction

The ellipsometer is a powerful tool for measuring the thickness and dielectric constants of thin films by analyzing the state of polarization (SOP) of reflected light. Features of ellipsometry include high resolution for thin films and independent determination of thickness and refractive index. Ellipsometry is currently used as a characterization technique for thin films in industries associated with semiconductors and flat-panel displays. The majority of commercially available ellipsometers require mechanical rotation of a polarizer or a wave plate [1], or electric phase modulation to measure the SOP of the reflected light. This causes optical modules and equipment as a whole to be large. On the other hand, static ellipsometers, or snapshot ellipsometers, are reported [2–6] that do not require either optical or electric modulation. Division-of-wavefront photopolarimeters [2] have a simple configuration and thus require no complicated alignment, unlike division-of-amplitude photopolarimeters [3–6]. However, the polarizers and wave plates used in Ref. 2 are discrete elements as large as several millimeters square.

We previously proposed and demonstrated a snapshot ellipsometer classified as a division-of-wavefront polarimeter utilizing an arrayed micropolarizer and an arrayed micro wave plate with a CCD camera [7]. Since a relay lens was used in that experiment to transfer the image of the arrayed elements to a CCD sensor, mechanical instability and interference caused by the lens remained as problems to solve. We report a compact static polarimeter module consisting of the arrayed optical elements attached directly to the CCD image sensor. We also demonstrate a portable ellipsometer using the polarimeter with high repeatability.

2. Principle

Figure 1 shows a schematic illustration of the proposed polarimeter module for the ellipsometer [1]. The receiver module is composed of an array of quarter wave plates, an array of polarizers, and a CCD image sensor that is used for analyzing the SOP. This module has no moving parts, and simultaneously acquires information equivalent to that obtained by conventional rotating element instruments. The SOP of the detected light is determined from images ob-

0003-6935/07/224963-05$15.00/0

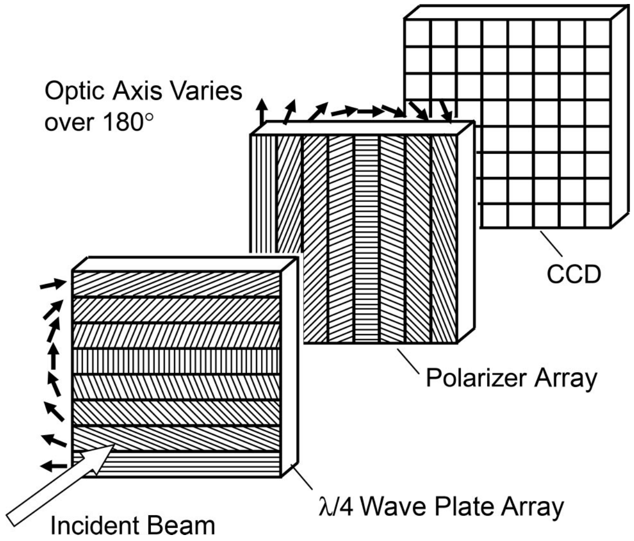

Fig. 1. Schematic illustration of the proposed polarimeter for the ellipsometer. For simplicity, the optical axis is shown as a 22.5° step over the range of 180°.

tained from the CCD sensor, and the film thickness and optical constants are immediately obtained.

This type of ellipsometer is characterized by compactness and a high level of repeatability, which are realized because there are no moving parts. There also is the potential to realize an ultracompact ellipsometer module integrating the optical source and receiver, suitable for deployment in a variety of manufacturing and measuring instruments.

The key elements are the arrayed polarizers and wave plates. As shown in Fig. 2, they are composed of photonic crystals; that is two-dimensional periodic structures of submicron periodicity. What we believe to be a unique structure of the photonic crystal elements is formed by depositing dielectric thin films on a grating substrate. Under a deposition process based on bias sputtering, known as autocloning [8], layers with a triangular corrugation are formed on the rectangular grating and are replicated layer by layer. By varying the stacking period L_1, the grating pitch L_2, and the number of layers, we can design polarizers and wave plates for an arbitrary operating wavelength [9–10].

The direction of the polarization extinguished by the polarizer and the fast axis of the wave plate both correspond to the direction of the substrate grating. Therefore, micropolarizers or wave plates with different optical axes can be monolithically integrated by patterning the substrate grating and one deposition process, as shown in Fig. 2. Compared with hybrid integration of discrete elements, monolithic integration has the advantages of precision of the orientation of the optical axes, sharpness of boundaries, and the possibility of a micron order precise unit.

3. Experiments

Polarizers and wave plates were designed and fabricated arrayed as follows. The width of each array is 50 μm and the optical axis varies by an 11.25° step over the range of 180° (11.25° = 180°/16). The initial gratings are formed on a silica substrate by electron beam lithography and reactive ion etching. The pitches of the grating for polarizers and wave plates are 300 and 200 nm, respectively. We selected Ta_2O_5 and SiO_2 as materials for the multilayer structure because they are transparent at the operating wavelength of 655 nm and have a high index contrast (2.2/1.45). The triangular corrugation is formed independently of the orientation. At the wavelength of 655 nm, the transmittance and extinction ratio of the polarizer are better than 95% and 35 dB, respectively, and the transmittance and retardation of the wave plate are better than 98% and 90 +\− 1° respectively.

The polarizer and wave-plate array are fixed to one another and diced to a chip of 2.8 mm × 3.8 mm. The optical axes of each array are varied in mutually orthogonal directions as illustrated. This chip is attached directly to a CCD image sensor with 1×10^6 pixels, as shown in Fig. 3. Since approximately 100 pixels of 4 μm square are included in a cell of a given polarizer orientation and wave-plate orientation, the signal-to-noise ratio is sufficient. A compact polarimeter module of 24 mm × 35 mm × 78 mm was produced including the driver and analog/digital (A/D) converter electronics.

Figures 4(a) and 4(b) show images acquired from the CCD sensor on detecting light beams with differ-

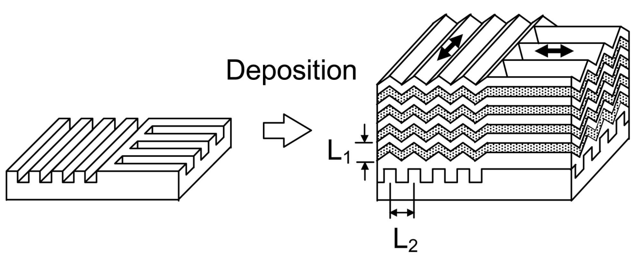

(a) (b)

Fig. 2. Arrayed polarizers and wave plates, which are composed of a two-dimensional periodic structure of submicron period. Arrows indicate the optical axes.

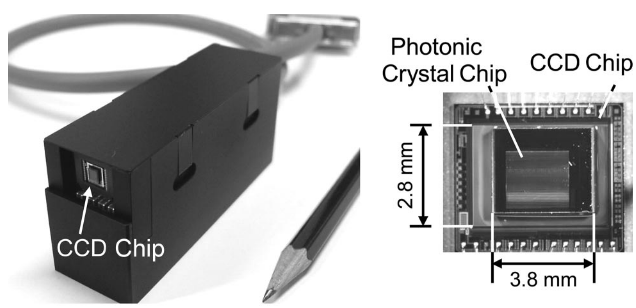

(a) (b)

Fig. 3. (a) A compact polarimeter module, (b) and an arrayed polarizer and arrayed wave plate attached to a CCD image sensor.

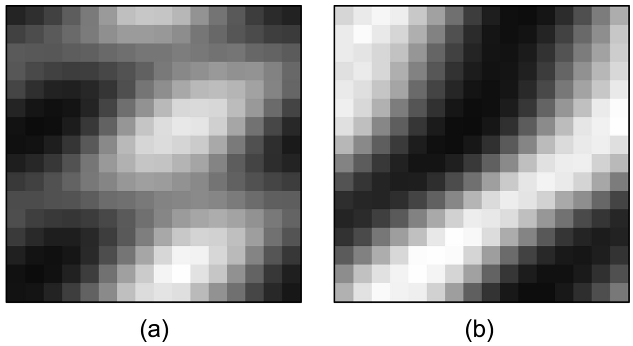

Fig. 4. Images outputted from the CCD sensor on detecting light beams of differing SOPs, (a) $\varepsilon = -0.018$, $\gamma = 23.8°$, and (b) $\varepsilon = -0.353$, $\gamma = -68.8°$.

ent SOPs. The axes of the polarizers vary along the horizontal direction, and those of the wave plates along the vertical direction. The second, third, and fourth terms of Eq. (1) are derived from two-dimensional Fourier transforms of the image, and thus the principal axis of the polarization ellipsoid γ and the ellipticity ε are obtained:

$$|u(\phi,\ \theta)|^2 = \frac{1}{2} + \frac{1}{4} \times \frac{1-\varepsilon^2}{1+\varepsilon^2}(1+\cos\alpha) \times \cos(2\phi - 2\gamma) + \frac{1}{4} \times \frac{1-\varepsilon^2}{1+\varepsilon^2}(1-\cos\alpha) \times \cos(4\theta - 2\phi - 2\gamma) + \frac{\varepsilon}{1+\varepsilon^2} \sin\alpha \cos(2\theta - 2\phi + \pi/2). \qquad (1)$$

Here, ϕ and θ are the orientations of the polarizer and quarter wave plate, and α is the retardation of the quarter wave plate. Before taking the Fourier transform, the intensity distribution of the incident light beam is compensated so that it will be flat by using a fitted Gaussian function, to reduce errors in the Fourier coefficients.

To confirm the operation of the polarimeter, measurement is performed by rotating a commercial polarizer or quarter wave plate placed between the light source and the polarimeter. Figure 5(a) indicates the relation between the measured γ and the azimuthal angle of a polarizer, while Fig. 5(b) indicates the relation between the measured ε and the azimuthal angle of a quarter wave plate. Both relations agree well with the theoretical curves, verifying sufficient accuracy for use of the module as a polarimeter.

Figure 6 shows an ellipsometer utilizing the above polarimeter. The angle of incidence is configurable by a pair of wedges of the desired angle. The footprint is A4 in size, and the weight is approximately 4 kg, which is one-tenth that of currently available ellipsometers. Several silicon dioxide films on Si wafer were measured at an angle of incidence of 60°. Light is launched into a polarization maintaining fiber from a laser diode light source, and collimated. Figure 7 shows simulated trajectories in the ε–γ plane as a function of the thickness of SiO_2 films deposited on Si

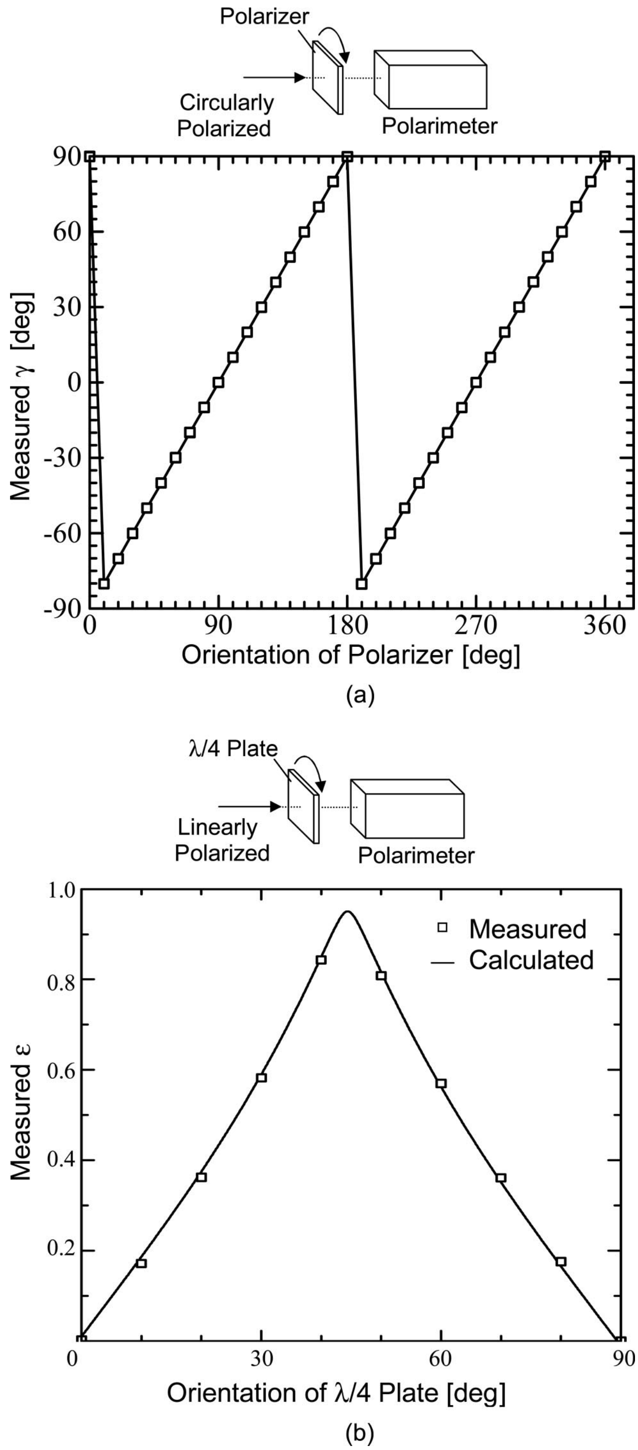

Fig. 5. (a) Relation between measured γ, the principal axis of the polarization ellipsoid, and the azimuthal angle of a polarizer. (b) Relation between the measured ellipticity ε and the azimuthal angle of a quarter wave plate.

wafer. The thickness and/or optical constants can be derived from the measured ε and γ in the same way that conventional ellipsometers use Ψ and Δ.

Figure 8 shows the correlation between the thickness measured by the ellipsometer reported here and the thickness as measured by a spectroscopic ellip-

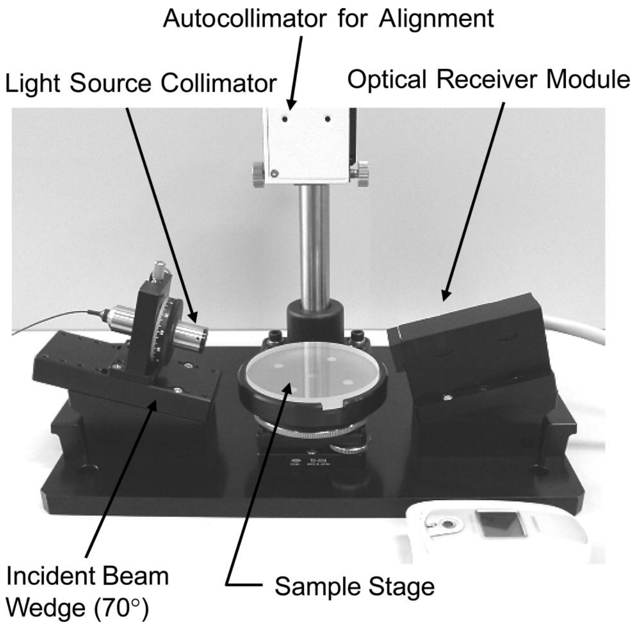

Fig. 6. Ellipsometer utilizing an arrayed polarizer and an arrayed wave plate. The footprint is reduced to A4, and the weight is as low as 4 kg.

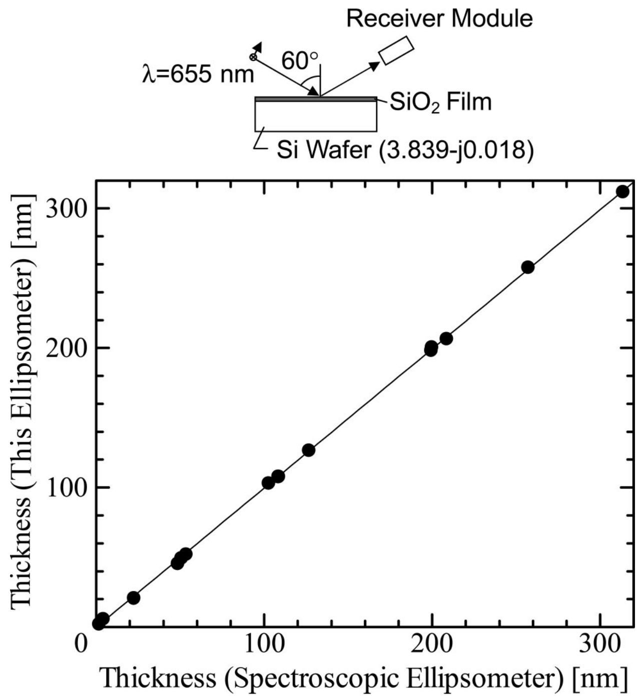

Fig. 8. Correlation between the thickness measured by the ellipsometer reported here and the exact thickness as measured by a spectroscopic ellipsometer.

someter (J. A. Woollam, M–2000). Over the range from 2 to 300 nm, the results agree well, indicating accurate operation of this ellipsometer. Figure 9 shows repeatability for a sample with a thickness of 126 nm and an n of 1.46. One hundred measured values obtained at an interval of 0.3 s are plotted. The speed of measurement mostly depends on the CCD sensor and electronic interface. It will be improved to less than 0.1 s by using the appropriate sensor and interface. The standard deviation of the thickness and refractive index are as low as 0.04 nm and 3×10^{-4}, respectively.

Next, the incident conditions were changed to attain the high resolution required for thin films. Here, the incident angle is set to 75°, which is close to Brewster's angle. The incident polarization is set at 10° from the plane of incidence to compensate for the difference between the reflection coefficients of

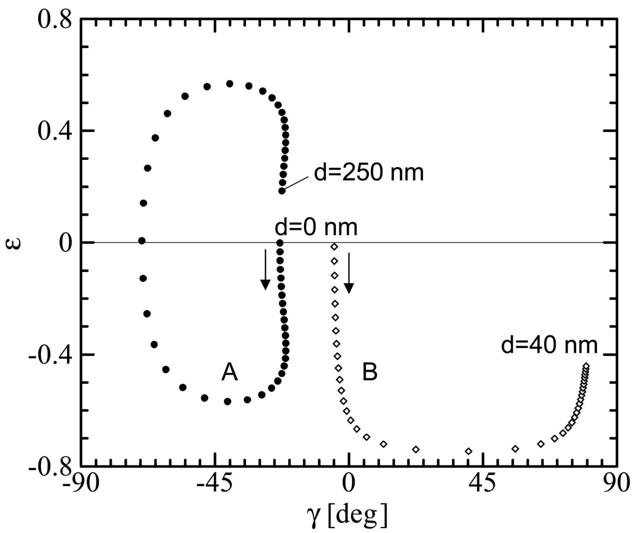

Fig. 7. Simulated trajectories in the ε–γ plane as a function of the thickness of SiO_2 film deposited on Si wafer. The angles of incidence for A and B are 60° and 75°, and the incident polarization for A and B are 45° and 10°, respectively. (The wavelength is 655 nm and the refractive index of SiO_2 at 655 nm is 1.456.)

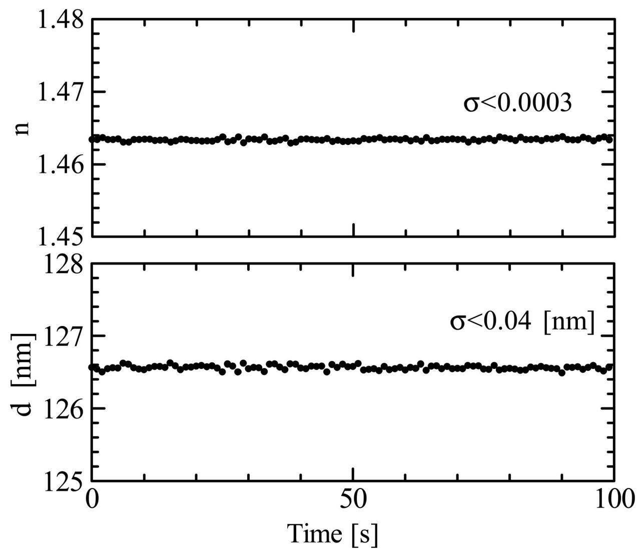

Fig. 9. Repeatability for a sample having a thickness of 126.6 nm and n of 1.463. One hundred measured values obtained at an interval of 0.3 s are plotted. The standard deviation of the thickness and n are as low as 0.04 nm and 3×10^{-4}, respectively.

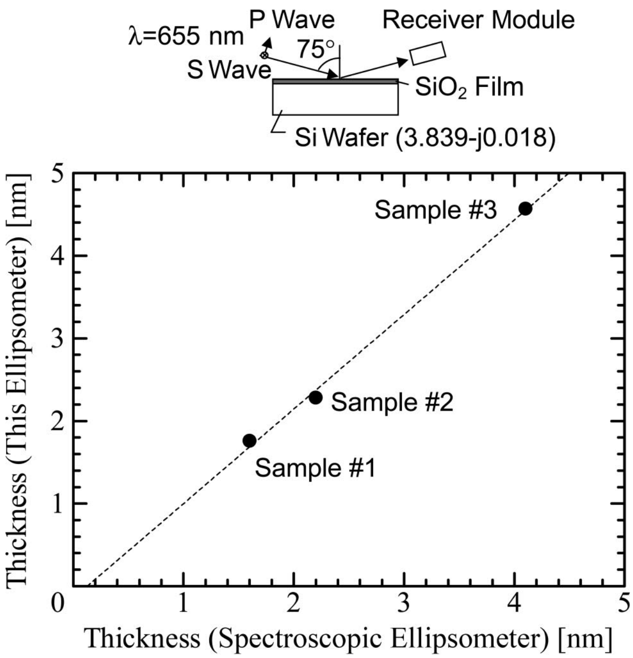

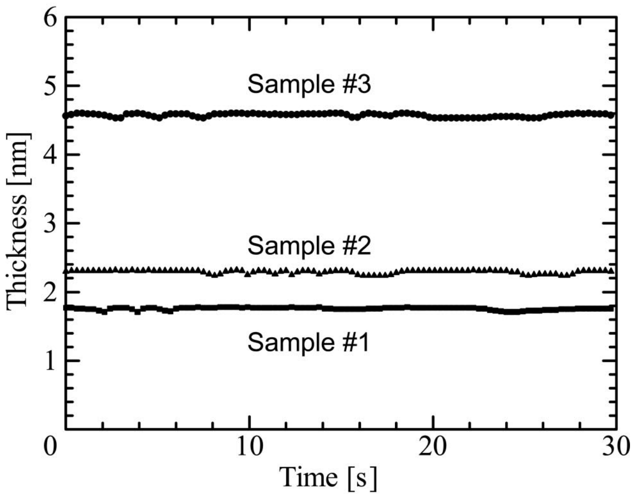

Fig. 10. (a) Correlation between thicknesses over the range from 1.6 to 4 nm measured by the ellipsometer reported here and exact thicknesses as measured by a spectroscopic ellipsometer. (b) One hundred measured values obtained at an interval of 0.3 s are plotted. The standard deviation of the thickness is as low as 0.03 nm.

the p- and s- waves. Figure 10(a) shows a good correlation between the thicknesses measured by the ellipsometer of this report and the thicknesses measured by a spectroscopic ellipsometer. The plotted data are the average values of 100 points. As shown in Fig. 10(b), the standard deviation is less than 0.03 nm. Thus a high resolution of 0.1 nm at an interval of 0.3 s is realized. These results demonstrate high resolution, good repeatability, and a measurement speed high enough for the majority of applications.

4. Conclusions

A compact ellipsometer utilizing an arrayed polarizer, an arrayed wave plate, and a CCD image sensor has been developed. A high level of repeatability and measurement speed high enough for most applications have been confirmed by measurement of SiO_2 films ranging from 2 to 300 nm in thickness deposited on an Si wafer. The next stage of research will focus on improvements to the module for use in manufacturing processes.

The authors thank M. Yamamoto of IMRAM, Tohoku University, for his valuable advice and comments.

References

1. R. M. A. Azzam and N. M. Bashara, *Ellipsometry and Polarized Light* (Elsevier, 1997).
2. E. Collett, "Determination of the ellipsometric characteristics of optical surfaces using nanosecond laser pulses," Surf. Sci. **96,** 156–167 (1980).
3. R. M. A. Azzam, "Light polarization: a rich source of information," Opt. Acta **29,** 685–689 (1982).
4. E. Masetti and M. P. de Silva, "Development of a novel ellipsometer based on a four-detector photopolarimeter," Thin Solid Films **246,** 47–52 (1994).
5. A. Kazama, Y. Yamada, T. Yamada, T. Oshige, T. Kaneko, and A. Nagamune, "Compact and high-speed ellipsometer," Proc. SPIE **1681,** 183 (1992).
6. Y. Kim, S. J. Kim, S. Y. Kim, S. H. An, D. Suh, J. Noh, S. M. Lee, K. H. P. Kim, W. Shin, and Y. Khang, "Experimental setup for *in situ* investigation of phase changing behavior in phase-change random-access memory medium by microfocusing nanosecond-time-resolved ellipsometry," Jpn. J. Appl. Phys., Part 1 **45,** 6452–6454 (2006).
7. T. Sato, Y. Sasaki, N. Hashimoto, and S. Kawakami, "Novel scheme of ellipsometry utilizing parallel processing with arrayed photonic crystal," Photonics Nanostruct. Fundam. Appl. **2,** 149–154 (2004).
8. S. Kawakami, "Fabrication of submicrometer 3D periodic structures composed of Si/SiO_2," Electron. Lett. **33,** 1260–1261 (1997).
9. Y. Ohtera, T. Sato, T. Kawashima, T. Tamamura, and S. Kawakami, "Photonic crystal polarization splitters," Electron. Lett. **35,** 1271–1272 (1999).
10. T. Sato, K. Miura, N. Ishino, Y. Ohtera, T. Tamamura, and S. Kawakami, "Photonic crystals for the visible range fabricated by autocloning technique and their application," Opt. Quantum Electron. **34,** 63–70 (2002).